Title
Applications of computational modeling in cardiac surgery.

Journal
Journal of cardiac surgery, 29(3)

ISSN
0886-0440

Authors
Lee, Lik Chuan
Genet, Martin
Dang, Alan B
et al.

Publication Date
2014-05-01

DOI
10.1111/jocs.12332

Peer reviewed

Published in final edited form as:
J Card Surg. 2014 May ; 29(3): 293–302. doi:10.1111/jocs.12332.

Applications of Computational Modeling in Cardiac Surgery

Lik Chuan Lee, PhD[1,2,3,4], **Martin Genet, PhD**[1,2,3,4], **Alan B. Dang, MD**[1,2,3,4], **Liang Ge, PhD**[1,2,3,4], **Julius M. Guccione, PhD**[1,2,3,4], and **Mark B. Ratcliffe, MD**[1,2,3,4]

[1]Department of Surgery, University of California, San Francisco, California

[2]Department of Bioengineering, University of California, San Francisco, California

[3]Department of Medicine, University of California, San Francisco, California

[4]Veterans Affairs Medical Center, San Francisco, California

Abstract

Although computational modeling is common in many areas of science and engineering, only recently have advances in experimental techniques and medical imaging allowed this tool to be applied in cardiac surgery. Despite its infancy in cardiac surgery, computational modeling has been useful in calculating the effects of clinical devices and surgical procedures. In this review, we present several examples that demonstrate the capabilities of computational cardiac modeling in cardiac surgery. Specifically, we demonstrate its ability to simulate surgery, predict myofiber stress and pump function, and quantify changes to regional myocardial material properties. In addition, issues that would need to be resolved in order for computational modeling to play a greater role in cardiac surgery are discussed.

Keywords

Computational modeling; Finite element method; Medical devices; Myocardial infarction

Introduction

Computational modeling (or computer simulation, mathematical modeling) is common in many areas of science and engineering. With the progressive increase in computing power, mathematical modeling has become an indispensable tool in scientific research and engineering product development of many industries, such as the automotive and aerospace industries.

Among the many benefits associated with the use of computational modeling, two key benefits stand out. First, computational modeling is versatile and can be used to probe the many “what if” scenarios without incurring the typical high costs associated with constructing new experiments. For example, once a computational model is created, the model can be used to quantify the relative contribution of each mechanism in the human

Corresponding Author: Mark B. Ratcliffe, MD, Division of Surgical Services (112), San Francisco Veterans Affairs Medical Center, 4150 Clement Street, San Francisco, California 94121. Telephone: (415) 221-4810. FAX: (415) 750-2181. Mark.Ratcliffe@va.gov.

heart towards some observed phenomenon. Second, computational modeling is particularly useful in quantifying results that are difficult or impossible to measure in experiments,.g. when the placement of accelerometers to measure vibrational response is difficult or impossible at certain locations in an automobile or aircraft.

Compared to its use in the automotive and aerospace industries, computational modeling in cardiology and cardiac surgery is in its infancy. This is primarily because living tissues, unlike metals and other engineering materials, have a complex microstructure and material behavior. Furthermore, material behavior of living tissues can evolve with time (i.e. the tissue can grow or hypertrophy) [1,2]. As a consequence, and due in part to the inherent difficulties in performing experiments on living tissues, constitutive stress-strain relationships of the myocardium are difficult to construct. Nevertheless, computational models of the heart have improved tremendously in the last several decades. To get a glimpse of this improvement, all one needs to do is to compare early computational models of the heart to the latest models. For example, one of the earliest computational models of the left ventricle (LV) was formulated with assumptions that the myocardial stress strain relationship is linear, non-directional (isotropic) and only undergoes small deformations. [3]. By comparison, a recent biventricular model was formulated using more accurate nonlinear myocardial stress-strain relationship with excitation-contraction coupling of the myocardium. Furthermore, tissue directionality is linked to arrangement of fiber in the myocardium (anisotropy[1]) and the model is based on large deformation theory [4].

With these improvements, computational modeling has been increasingly applied to problems in cardiac surgery over the past decade. These applications range from elucidating the effects of various heart diseases to predicting the effects of clinical interventions. The goal of this article is to demonstrate the specific capabilities of computational cardiac modeling using various examples, specifically, its ability to simulate surgery, predict myofiber stress and pump function, and quantify changes to myocardial material properties.

Computational Modeling

Computational Cardiac Mechanics

Computational cardiac mechanics is at the intersection of three scientific domains: continuum mechanics, materials science and numerical methods (Fig. 1a). Continuum mechanics is the basic reference framework of mechanical engineering that was developed with the expansion of engineering [5]. Continuum mechanics is based upon the hypothesis that matter is continuous. This is, of course, not exactly true. However, this hypothesis is often very realistic and provides an adequate description of the deformation of matter through the equilibrium equations that all matters must satisfied. These equilibrium equations are derived from basic conservation laws, specifically, the conservation of mass, momentum, energy. They are general and apply to all types of materials, be it ceramics, metals or living tissues.

[1]Anisotropy, as opposed to isotropy where the material response is independent of the direction, implies that the material response is direction-dependent.

The material or constitutive stress-strain relationship is specific for a given material. This relationship describes how much force is developed when the material is stretched or strained, or the converse. Simply put, the constitutive stress-strain relationship describes the material mechanical behavior. Many different constitutive stress-strain relationships have been formulated for cardiac tissues and they all share the key features of having a nonlinear and anisotropic relationship, and having the ability to contract in the muscle fiber direction when stimulated. Due to its simplicity, we have mostly used the constitutive stress-strain relationships formulated by Guccione et al. [7, 8] in our models which were validated in clinically-relevant large animal studies.

Combining the equations from continuum mechanics and constitutive stress-strain leads to a set of (coupled partial differential) equations. The displacement/strain/stress at every material point within the heart wall and every time point during the cardiac cycle can be found once these coupled equations are solved. However, these equations usually cannot be solved analytically for real heart geometries and loading; and its solution can only be found for a few specialized cases with idealized heart geometry. Therefore, one is forced to look for approximate solutions for this set of equations.

Numerical methods, which form the last pillar of computational cardiac mechanics, are often used to approximate systems of differential equations. Although many numerical methods can be used to approximate systems of equations in cardiac mechanics, the most widely used method is the finite element (FE) method. The popularity of the FE method is largely due to its versatility, performance and solid theoretical foundation (e.g. proof of convergence, error control, etc.). The main idea behind the FE method (and in all numerical methods) is to split the original continuous problem into a discrete one, a process typically known as “discretization”. To achieve that, the FE method splits the material domain (structure) into many subparts called elements whose vertices are called nodes. Together, the nodes and elements form the mesh that is typically known as an FE mesh (Fig. 1b). In the FE method, the approximate solution is expressed as the weighted sum of a finite number of known functions called shape functions. One shape function is associated with each node and the shape function is usually chosen to be linear within each element; though higher order shape functions (such as quadratic shape functions) can also be used. The weights associated with each shape function are derived to obtain the best possible approximation with that particular set of shape functions. The result is a large system of algebraic equations that can be solved most efficiently with computers.[2]

For the interested readers, we have provided a more simplified description of the FE method in relation to the three abovementioned domains in the Appendix.

Finite element over Laplace’s law to calculate ventricular wall stress

Given the popularity of using Laplace’s law to calculate ventricular wall stress among clinicians, it is worthwhile to examine some of the key merits of using the FE method over

[2]When the system of algebraic equations is nonlinear, these equations are typically turned into a series of linear equations or “linearized” or before solving with a computer. The most commonly used method for this “linearization” is the Newton-Raphson method

Laplace's law. Certainly, there must exist some very good reasons why the FE method should be preferred over Laplace's law, especially since the FE method is much more complicated and requires significantly more effort than Laplace's law [8].

The key advantage of the FE method over Laplace's law is its versatility. For instance, once the stress-strain relationship is validated, the FE method can be used to calculate regional stresses in any arbitrary geometry and under any arbitrary load(s). In contrast, Laplace's law was formulated based on the restrictive assumption of a thin ventricular wall, where the law (in its simplest form) states that the ventricular wall stress is directly proportional to the ventricular cavity pressure and endocardial radius of curvature, and is inversely proportional to the ventricular wall thickness. As a consequence, stress is uniform across the ventricular wall. Laplace's law therefore can only calculate average stresses across the ventricular wall. Because the ventricular wall is inhomogeneous with muscle fiber orientation varying across the wall thickness [9], the use of Laplace's law to quantify forces acting or generated by the muscle fiber (i.e. myofiber stress) is bound to be erroneous. To illustrate this, Zhang et al. [10] recently compared stresses in an infarcted sheep LV calculated from the FE method to that calculated from Laplace's law. Not only did they find that Laplace's law severely underestimated the average myofiber stress in both remote (by 64%) and borderzone (BZ) region (by 35%) at end-systole (ES) when compared to the FE method, they also found a significant disparity in stress predicted by the two methods when used to study the effects of the Dor procedure. Being more general and without any restrictive assumptions other than the validity of the material constitutive law, the FE method is clearly more accurate. Hence, caution should be exercised when using Laplace's law to quantify myofiber stress.

The other advantage of the FE method is that it has a more extensive predictive capability than Laplace's law, whose only utility is in ventricular stress estimation. Not only does it predict regional stresses more accurately, it can also be used to predict material deformation that is impossible to do using Laplace's law. This predictive capability enables other metrics of cardiac function, such as stroke volume and regional myocardial strains, to be quantified. Moreover, clinical interventions and the effects due to the progression of heart diseases can also be simulated realistically using the FE method. All these capabilities make the FE method a potentially powerful tool with high clinical value.

Application in Cardiac Surgery

With the advancement in experimental techniques to quantify myocardial material response, and imaging techniques that not only make it possible to construct accurate patient-specific ventricular geometry but is also capable of measuring *in vivo* myocardial deformation, computational cardiac modeling has become more applicable to clinical use. Indeed, computational cardiac modeling has increasingly been used to elucidate the effects of various heart diseases and clinical interventions. We now demonstrate four specific capabilities of computational cardiac modeling.

Prediction of myofiber stress

Since elevated myofiber stress is widely believed to be responsible for adverse cardiac remodeling [11], knowledge of the *in vivo* regional myofiber stress should shed light on the

prognosis of heart diseases in patients. Laplace's law is often used to estimate ventricular myofiber stress. However, as mentioned earlier, the accuracy of Laplace's law is limited by the restrictive assumptions associated with it, and the myofiber stress predicted by this method can be significantly different from that predicted using a more general FE method [10]. Thus, the FE method should be used to estimate ventricular myofiber stress when available. Such was the case in a study of the Cardiokinetix Parachute device [12].

In this analysis, the FE method was used to analyze the effects of the Parachute® developed by CardioKinetix Inc (Menlo Park, CA) that is intended to reverse LV remodeling after antero-apical myocardial infarction (MI). This device consists of an expanded polytetrafluoroethylene (ePTFE) membrane bonded to an expanded Nitinol frame consisting of 16 struts. The Nitinol frame is attached to a radioplaque foot. In the deployment process, the device is first collapsed and then delivered percutaneously from the femoral artery by standard catheterization techniques. Once in position, the Parachute device is expanded and the anchor tip of each strut engages and hooks on to the LV endocardial wall. In the final deployed configuration, the Parachute device partitions the LV into an upper and a lower chamber (Fig. 2a).

Treatment using this device has been shown to lead to a reduction in LV end-diastolic (ED) volume and ES volume in both animals [13] and humans [14] but the mechanism that led to these improvements is unclear. To elucidate its effects, an FE model of the LV implanted with the Parachute® device was constructed. This model is realistic, in particular because 1) the FE LV model was reconstructed from CT images of a patient before Parachute device implantation and 2) the deployment process was simulated in addition to the ED and ES phases (Fig. 2b).

The main result of this simulation is that treatment using the Parachute device leads to a substantial reduction in ED myofiber stress. The ES myofiber stress, by comparison, was predicted to be slightly changed after implantation. Specifically, the average ED myofiber stress was predicted to be 30% lower than that before treatment with the bulk of that reduction coming from the partitioned lower chamber of the LV (Fig. 2c). The results from this single-patient study suggest that the reported therapeutic effects arising from Parachute device treatment may be an outcome of a reduction in ED myofiber stress. These results are preliminary and studies involving more patients are required to confirm this result.

Prediction of pump function

The ability of the FE method to calculate both end-diastolic and end-systolic pressure volume relationships (compliance and elastance respectively) allows the calculation of ventricular pump function, which is impossible to do using Laplace's law. This capability was demonstrated in an analysis of the Acorn CorCap Cardiac Support Device (CSD) (Acorn Cardiovascular Inc, St. Paul, MN) using the FE method [15].

The Acorn CSD is a bidirectional woven polyester yarn jacket that is implanted to the epicardial ventricular wall. This device can be classified under a larger class of devices commonly referred to as a cardiac passive restraint device. Other such devices include the Paracor HeartNet (Paracor Medical, Sunnyvale, CA) device [16] and the adjustable

ventricular restraint device [17]. The primary aim of the restraint device is to reduce elevated ventricular wall stress that is associated with progressive ventricular dilation by mechanically restraining the ventricles. It is hypothesized that doing so will halt or even reverse the adverse ventricular remodeling process.

In this analysis, the mechanical effects of Acorn CSD were simulated using a FE model of a dog biventricular unit with induced dilated cardiomyopathy from rapid pacing (Fig. 3a). A prior FE LV model has also been used to simulate the effects of passive restraint device [18] but that model is highly idealized because it assumed that the LV is a prolate spheroid and the effects of the device is equivalent to that of a constant pressure applied to the epicardium. The biventricular FE model is not restricted by any of these assumptions. In addition, the effects of pre-stretch of the Acorn CSD was also modeled to address the issue on how tight the Acorn CSD needs to be when it is implanted to the epicardial wall; since all that was mentioned in previous studies is that the CSD has to be fitted “snugly” [19].

The results from the simulation show that even though the Acorn CSD can reduce the ED myofiber stress substantially (by as large as 78%), and more so with pre-stretch, this huge reduction in myofiber stress was always accompanied by a decrease in diastolic compliance. Consequently, both LV and RV ED pressure-volume relationships were shifted to the left by 7% without pre-stretch and 11% with pre-stretch (Fig. 3b). Because the LV and RV end-systolic pressure-volume relationships were predicted to be insensitive to the presence of Acorn CSD, the Starling’s relationship became more depressed and stroke volume was reduced by 23% (without pre-stretch) and 30% (with pre-stretch) (Fig. 3c). Thus, it would be impossible to address the possibility of the Acorn CSD in depressing the ventricular pump function if Laplace’s law was used in place of the FE method to evaluate this device.

Inverse prediction of myocardial material parameters

The FE method can also be used to calculate tissue material parameters by comparing experimentally measured material/ structural deformation with FE calculated deformation and adjusting material parameters until the two are similar. This capability allows one to track the evolution of heart disease and to quantify the effect of a cardiac device or operation on regional diastolic and systolic material parameters.

Earlier attempts to quantify regional ventricular material properties were performed using *ex vivo* biaxial tissue-stretching experiments [20]. The ability to quantify regional ventricular material properties *in vivo* was made possible when medical imaging techniques capable of measuring *in vivo* myocardial strain noninvasively (e.g. tagged MR imaging) were introduced and combined with the FE method. This methodology was applied in earlier works that quantified *in vivo* passive (or diastolic) myocardial materials properties [21, 22] and in understanding the mechanical dysfunction of the LV borderzone [23, 24]. More recently, this methodology was also applied to quantify the effects of clinical interventions such as the bioinjection therapy [25] and the Dor procedure [26]. The latter is now described in greater detail.

The Dor procedure (also known as the endoventricular patch plasty procedure) is a surgical procedure used to reduce the LV volume after MI and subsequent LV remodeling. The

primary aim of this procedure is to reduce LV wall stress, which is associated to the LV volume according to Laplace's law [27]. It has also been suggested that the Dor procedure may help reduce BZ stress and strain that would improve myocardial contractility at the BZ [28].

To quantify the effects of the Dor procedure on regional contractility and myofiber stress, five MRI-reconstructed FE models of the sheep LV were created at 3 different time points in this study, namely, 2 weeks before surgery, 2 weeks after surgery and 6 weeks after surgery. Based on MR images, the dyskinetic infarct, the BZ and the remote regions were identified and delineated in the LVs as distinct material regions, each with a different contractility reflected by a material parameter of the constitutive law (Fig. 4a). Regional myocardial strain was also measured non-invasively using tagged MRI at these time points. In these FE models, the regional material parameter associated with the tissues contractility were adjusted in a systematic way using the computational optimization method so as to minimize the difference between the FE-predicted and the MR-measured 3-dimensional systolic myocardial strain and the LV cavity volume at ED and ES [29]. Myofiber stress in these sheep models was calculated based on the set of "optimized" material parameters.

Contrary to the hypothesis that BZ contractility would improve after the Dor procedure, this study found that the BZ contractility remained depressed when compared to the remote region. Not only did the BZ contractility failed to improve after the Dor procedure, the study also found that the remote region's contractility has decreased by 24% after the procedure (Fig. 4b). These findings occurred in spite of the fact that the calculated myofiber stress at ED and ES decreased after the Dor procedure (Fig. 4c). Interestingly, the Surgical Treatment for Ischemic Heart Failure (STICH) trial concluded that adding the Dor procedure to coronary artery bypass grafting adds no benefits [30]. This result is controversial in that other clinical studies have found that such a procedure can benefit patients [31]. Given that there are other kinds of variants of the Dor procedure (e.g. the Pacopexy technique [32]), computational modeling, as shown in this study, can be both useful and efficient in providing an insight to the regional pathological changes of the ventricles associated with such procedures and possibly help to determine which patients may benefit most from volume reduction surgery.

Simulation of surgery

Finally, the FE method can be used to simulate surgery and hence, can potentially be used for surgery planning. The key to this last capability lies in the method's ability to simulate the suturing process, as was demonstrated in our two recent analyses of mitral annuloplasty [26, 27].

Finite element modeling has been used extensively to model mitral regurgitation [35], study the effects of the mitral annuloplasty [36–40], quantify the material properties of mitral valve leaflets *in vivo* using methodology similar to that described in the previous section [41] and perform stress analysis on the mitral valve leaflets [42,43]. However, the mitral valve apparatus is usually isolated from the LV and studied individually in all these studies.

Recently, our group created the first FE model of the mitral valve incorporated into an animal-specific infarcted LV [11]. This model contains most of the structural components found in a complete LV-mitral-valve assembly. The model contains the mitral valve leaflets, the chordae tendinae, the papillary muscles and the LV, which are all connected to one another in an anatomically realistic fashion (Fig. 5a).

Building on this model, Wong et al. [34] investigated the effects of mitral annuloplasty shape in ischemic mitral regurgitation by virtually suturing two different shaped mitral annuloplasty rings, namely, a saddle-shape and an asymmetric-shape (Fig. 5b), to the mitral annulus of the model. The virtual sutures were modeled using two-node “beam” elements with one end attached to the annuloplasty ring and the other attached to the mitral annulus (Fig. 5c). An axial tension was then prescribed in each “suture” element so that its two ends were “pulled” towards each other. As a result, the mitral annulus was pulled towards the annuloplasty ring until the annulus conformed to the ring shape.

The principal findings of this study were that the effects of mitral annuloplasty are generally insensitive to the shape of the annuloplasty ring such that both septolateral distance and coaptation of the mitral leaflets were improved with implantation of these two types of annuloplasty rings (Fig. 5d). The modeling of sutures as described in this study should in principle also enable the FE method to be used for planning and/or optimizing other cardiac surgical procedures.

Implementation

On the other hand, several issues need to be resolved in order for computational modeling to play a greater role in cardiac surgery, especially in patient-specific computational modeling. It is useful to consider the issues in three different categories: software, hardware, and implementation.

Software Issues

First, the construction of a patient-specific FE model is generally time-consuming and requires technical expertise. There are no automatic image contouring and segmentation tools suitable for FE modeling and current semi-automatic methods require the user to spend several hours or even days to generate a patient-specific FE model. However, workarounds may be possible. For instance, one way to speed up model creation is to have a library of models where an existing template is morphed into an anatomically correct model using key anatomical landmarks. Also, it may be possible to develop a web or cloud based software tool or system where the end user uploads imaging data, semi-automatic model creation occurs on the client side with the help of a super user, and model images and results are transmitted over the web to the end user for viewing.

Second, current constitutive laws of cardiac tissues were for the most part based on *ex vivo* experimental tests and may not reflect the *in vivo* situation. A key point is that a constitutive law describing growth in living cardiac tissues has not been experimentally validated (although several such laws have been proposed). Technically, therefore, current computational models can only be used to study the acute effects of diseases and clinical

interventions. Third, microstructure of the cardiac tissues (e.g. myofiber orientation in the ventricular walls) can only be measured in the explanted heart via invasive histological measurements or non-invasive diffusion tensor imaging. As such, current ventricular models are not "microstructurally" patient-specific although they are "geometrically" patient-specific. It is only very recently that *in vivo* measurement of myofiber orientation with diffusion tensor imaging has become possible although the total scan time of 10 – 15 minutes per image slice [48] may still be challenging for heart failure patients.

Hardware Issues

High resolution FE analysis is computationally expensive. Although current high-end consumer desktop computer has sufficient computing power to perform FE analysis, it may take several hours to days to calculate model deformation and results. This is not an issue for research or teaching purposes but may not be adequate for surgical or procedural planning due to pre-procedure time constraints.

As discussed with software above, cloud based systems may also be the solution to hardware issues. Many hospitals currently have a cluster of servers used to handle the computational workload of a hospital during peak operating hours. After hours, unused computational resources could be redirected toward pre-operative planning. Another alternative resource is the on-demand web or cloud based software tool discussed above would allow end users access to high end computer clusters running under dedicated super user supervision.

Implementation Issues

Once software and hardware issues are overcome, implementation issues will be present. First, as with all new technologies introduced in medicine, cost effectiveness must be established. Second, users must be trained to use this technology. Like all new technologies, this will likely start with courses intended for practicing clinicians in tertiary-referral centers where trainees will be exposed to the technology.

With time and increased clinical evidence of utility and cost effectiveness as well as decreased costs, patient specific FE modeling will be used in routine care. The next issue is whether these FE studies will be performed and interpreted by radiologists, cardiologists or surgeons. We believe that a multidisciplinary approach will ultimately be adopted. MRI appears to be the optimal modality for acquiring patient-specific anatomy and involving the radiologist to optimize the scanning parameters will be important. As patient-specific computational modeling can be used to evaluate optimal strategies for both traditional open cardiac surgery as well as interventional methods, one would imagine that both cardiologists and cardiac surgeons would be users of this technology. As computational modeling expands beyond acute biomechanical evaluation and can simulate growth in living cardiac tissues as well as response to pharmacologic interventions, the users of patient specific computational modeling will increase.

Conclusion

We have demonstrated four capabilities of computational cardiac modeling, namely, its ability to simulate surgery, predict myofiber stress and pump function, and quantify changes

to myocardial material properties. In this review, we have offered only a glimpse of the potentially huge role that computational modeling can play in cardiac surgery. There are many other cardiac surgical areas where computational modeling have been applied. Some of these areas include (but are not limited to) stress analysis of aortic aneurysms [44, 45] and the analysis of blood flow using computational fluid dynamics after Coronary Artery Bypass Grafting [46] and for quantifying fractional flow reserve [47]. We foresee that in time, computational modeling will become an indispensable tool in accelerating the development of effective medical treatments and in improving patient care. Patient-specific computational modeling may even form the basis for clinical decision making. We suggest that the future of computational modeling in cardiac surgery remains bright with huge potential to be reaped.

Acknowledgments

This study was supported by NIH grants R01-HL-063348 and R01-HL-084431 (Dr. Ratcliffe); R01-HL-077921 and R01-HL-118627 (Dr. Guccione); and by a Marie-Curie international outgoing fellowship within the 7th European Community Framework Program (Dr. Genet).

References

1. Fung YC. Stress, strain, growth, and remodeling of living organisms. Z Angew Math Phys. 1995:S469–82.
2. Humphrey JD. Review Paper: Continuum biomechanics of soft biological tissues. Proc R Soc A Math Phys Eng Sci. 2003; 459:3–46.
3. Janz RF, Grimm AF. Finite-Element Model for the Mechanical Behavior of the Left Ventricle: Prediction of Deformation in the Potassium-arrested Rat Heart. Circ Res. 1972; 30:244–52. [PubMed: 5061321]
4. Wall ST, Guccione JM, Ratcliffe MB, et al. Electromechanical feedback with reduced cellular connectivity alters electrical activity in an infarct injured left ventricle: a finite element model study. Am J Physiol Heart Circ Physiol. 2012; 302:H206–14. [PubMed: 22058157]
5. Fung, YC. A first course in continuum mechanics. Englewood Cliffs, NJ: Prentice Hall; 1977.
6. Guccione JM, Waldman LK, McCulloch AD. Mechanics of active contraction in cardiac muscle: part II-cylindrical models of the systolic left ventricle. J Biomech Eng. 1993; 115:82–90. [PubMed: 8445902]
7. Guccione JM, Costa KD, McCulloch AD. Finite element stress analysis of left ventricular mechanics in the beating dog heart. J Biomech. 1995; 28:1167–77. [PubMed: 8550635]
8. Yin FC. Ventricular wall stress. Circ Res. 1981; 49:829–42. [PubMed: 7023741]
9. Streeter DD, Spotnitz HM, Patel DP, et al. Fiber orientation in the canine left ventricle during diastole and systole. Circ Res. 1969; 24:339–47. [PubMed: 5766515]
10. Zhang Z, Tendulkar A, Sun K, et al. Comparison of the Young-Laplace law and finite element based calculation of ventricular wall stress: implications for postinfarct and surgical ventricular remodeling. Ann Thorac Surg. 2011; 91:150–56. [PubMed: 21172505]
11. Grossman W. Cardiac hypertrophy: useful adaptation or pathologic process? Am. J Med. 1980; 69:576–84.
12. Lee LC, Ge L, Zhihong Z, et al. Patient-specific finite element modeling of the Cardiokinetix Parachute® device: Effects on left ventricular wall stress and function. Med Biol Eng Comput. 2014 (In press);
13. Nikolic SD, Khairkhahan A, Ryu M, et al. Percutaneous implantation of an intraventricular device for the treatment of heart failure: experimental results and proof of concept. J Card Fail. 2009; 15:790–97. [PubMed: 19879466]

14. Sagic D, Otasevic P, Sievert H, et al. Percutaneous implantation of the left ventricular partitioning device for chronic heart failure: a pilot study with 1-year follow-up. Eur J Hear Fail. 2010; 12:600–606.
15. Wenk JF, Ge L, Zhang Z, et al. Biventricular Finite Element Modeling of the Acorn CorCap Cardiac Support Device on a Failing Heart. Ann Thorac Surg. 2013; 95:2022–27. [PubMed: 23643546]
16. Magovern JA. Experimental and clinical studies with the Paracor cardiac restraint device. Semin Thorac Cardiovasc Surg. 2005; 17:364–68. [PubMed: 16428045]
17. Ghanta RK, Rangaraj A, Umakanthan R, et al. Adjustable, physiological ventricular restraint improves left ventricular mechanics and reduces dilatation in an ovine model of chronic heart failure. Circulation. 2007; 115:1201–10. [PubMed: 17339543]
18. Jhun CS, Wenk JF, Zhang Z, et al. Effect of adjustable passive constraint on the failing left ventricle: A finite element model study. Ann Thorac Surg. 2010; 89:132–37. [PubMed: 20103222]
19. Oz MC, Konertz WF, Kleber FX, et al. Global surgical experience with the Acorn cardiac support device. J Thorac Cardiovasc Surg. 2003; 126:983–91. [PubMed: 14566236]
20. Gupta KB, Ratcliffe MB, Fallert MA, et al. Changes in passive mechanical stiffness of myocardial tissue with aneurysm formation. Circulation. 1994; 89:2315–26. [PubMed: 8181158]
21. Moulton MJ, Creswell LL, Actis RL, et al. An inverse approach to determining myocardial material properties. J Biomech. 1995; 28:935–48. [PubMed: 7673261]
22. Moulton MJ, Creswell LL, Downing SW, et al. Myocardial material property determination in the in vivo heart using magnetic resonance imaging. Int J Card Imaging. 1996; 12:153–67. [PubMed: 8915716]
23. Moulton MJ, Downing SW, Creswell LL, et al. Mechanical dysfunction in the border zone of an ovine model of left ventricular aneurysm. Ann Thorac Surg. 1995; 60:986–97. [PubMed: 7575006]
24. Guccione JM, Moonly SM, Moustakidis P, et al. Mechanism underlying mechanical dysfunction in the border zone of left ventricular aneurysm: a finite element model study. Ann Thorac Surg. 2001; 71:654–62. [PubMed: 11235723]
25. Wenk JF, Eslami P, Zhang Z, et al. A novel method for quantifying the in-vivo mechanical effect of material injected into a myocardial infarction. Ann Thorac Surg. 2011; 92:935–41. [PubMed: 21871280]
26. Sun K, Zhang Z, Suzuki T, et al. Dor procedure for dyskinetic anteroapical myocardial infarction fails to improve contractility in the border zone. J Thorac Cardiovasc Surg. 2010; 140:233–9. 239.e1–4. [PubMed: 20299030]
27. Menicanti L, Di Donato M. The Dor procedure: What has changed after fifteen years of clinical practice? J Thorac Cardiovasc Surg. 2002; 124:886–90. [PubMed: 12407369]
28. Ratcliffe MB. Non-Ischemic Infarct Extension: A New Type of Infarct Enlargement and a Potential Therapeutic Target. J Am Coll Cardiol. 2002; 40:1168–71.
29. Sun K, Stander N, Jhun CS, et al. A computationally efficient formal optimization of regional myocardial contractility in a sheep with left ventricular aneurysm. J Biomech Eng. 2009; 131:111001. [PubMed: 20016753]
30. Jones RH, Velazquez EJ, Michler RE, et al. Coronary Bypass Surgery with or without Surgical Ventricular Reconstruction. N Engl J Med. 2009; 360:1705–17. [PubMed: 19329820]
31. Buckberg G, Athanasuleas C, Conte J. Surgical ventricular restoration for the treatment of heart failure. Nat Rev Cardiol. 2012; 9:703–16. [PubMed: 23149831]
32. Isomura T, Horii T, Suma H, et al. Septal anterior ventricular exclusion operation (Pacopexy) for ischemic dilated cardiomyopathy: treat form not disease. Eur J Cardiothorac Surg. 2006; 29 (Suppl 1):S245–50. [PubMed: 16567109]
33. Wenk JF, Zhang Z, Cheng G, et al. First finite element model of the left ventricle with mitral valve: insights into ischemic mitral regurgitation. Ann Thorac Surg. 2010; 89:1546–53. [PubMed: 20417775]
34. Wong VM, Wenk JF, Zhang Z, et al. The effect of mitral annuloplasty shape in ischemic mitral regurgitation: a finite element simulation. Ann Thorac Surg. 2012; 93:776–82. [PubMed: 22245588]

35. Kunzelman KS, Reimink MS, Cochran RP. Annular dilatation increases stress in the mitral valve and delays coaptation: a finite element computer model. Cardiovasc Surg. 1997; 5:427–34. [PubMed: 9350801]
36. Kunzelman KS, Reimink MS, Cochran RP. Flexible versus rigid ring annuloplasty for mitral valve annular dilatation: a finite element model. J Heart Valve Dis. 1998; 7:108–16. [PubMed: 9502148]
37. Votta E, Maisano F, Bolling SF, et al. The Geoform disease-specific annuloplasty system: a finite element study. Ann Thorac Surg. 2007; 84:92–101. [PubMed: 17588392]
38. Rausch MK, Bothe W, Kvitting JPE, et al. Mitral valve annuloplasty: a quantitative clinical and mechanical comparison of different annuloplasty devices. Ann Biomed Eng. 2012; 40:750–61. [PubMed: 22037916]
39. Bothe W, Kvitting J-PE, Stephens EH, et al. Effects of different annuloplasty ring types on mitral leaflet tenting area during acute myocardial ischemia. J Thorac Cardiovasc Surg. 2011; 141:345–53. [PubMed: 21241857]
40. Bothe W, Rausch MK, Kvitting JPE, et al. How do annuloplasty rings affect mitral annular strains in the normal beating ovine heart? Circulation. 2012; 126:S231–8. [PubMed: 22965988]
41. Krishnamurthy G, Ennis DB, Itoh A, et al. Material properties of the ovine mitral valve anterior leaflet in vivo from inverse finite element analysis. Am J Physiol Heart Circ Physiol. 2008; 295:H1141–H1149. [PubMed: 18621858]
42. Xu C, Jassar AS, Nathan DP, et al. Augmented mitral valve leaflet area decreases leaflet stress: a finite element simulation. Ann Thorac Surg. 2012; 93:1141–45. [PubMed: 22397985]
43. Xu C, Brinster CJ, Jassar AS, et al. A novel approach to in vivo mitral valve stress analysis. Am J Physiol Heart Circ Physiol. 2010; 299:H1790–4. [PubMed: 20952665]
44. Shang EK, Nathan DP, Sprinkle SR, et al. Peak wall stress predicts expansion rate in descending thoracic aortic aneurysms. Ann Thorac Surg. 2013; 95:593–98. [PubMed: 23245445]
45. Shang EK, Nathan DP, Woo EY, et al. Local wall thickness in finite element models improves prediction of abdominal aortic aneurysm growth. J Vasc Surg. 2013:1–7.
46. Sankaran S, Esmaily Moghadam M, Kahn AM, et al. Patient-specific multiscale modeling of blood flow for coronary artery bypass graft surgery. Ann Biomed Eng. 2012; 40:2228–42. [PubMed: 22539149]
47. Taylor CA, Fonte TA, Min JK. Computational fluid dynamics applied to cardiac computed tomography for noninvasive quantification of fractional flow reserve: scientific basis. J Am Coll Cardiol. 2013; 61:2233–41. [PubMed: 23562923]
48. Toussaint N, Stoeck CT, Schaeffter T, et al. In vivo human cardiac fibre architecture estimation using shape-based diffusion tensor processing. Med Image Anal. 2013; 17:1243–55. [PubMed: 23523287]

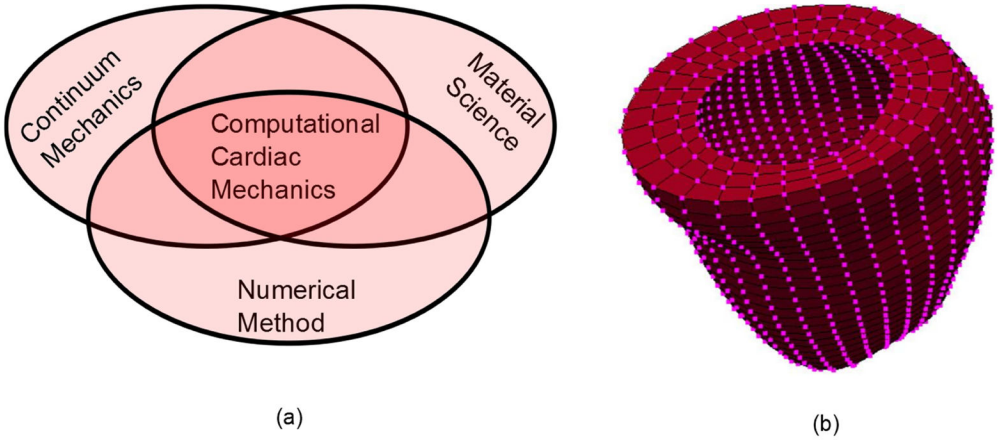

Figure 1.

(a): Computational cardiac mechanics as an intersection of three domains: continuum mechanics, materials science and numerical method. **(b):** A FE mesh of a LV. The elements (demarcated by the black lines) are inter-connected through nodes (shown in pink).

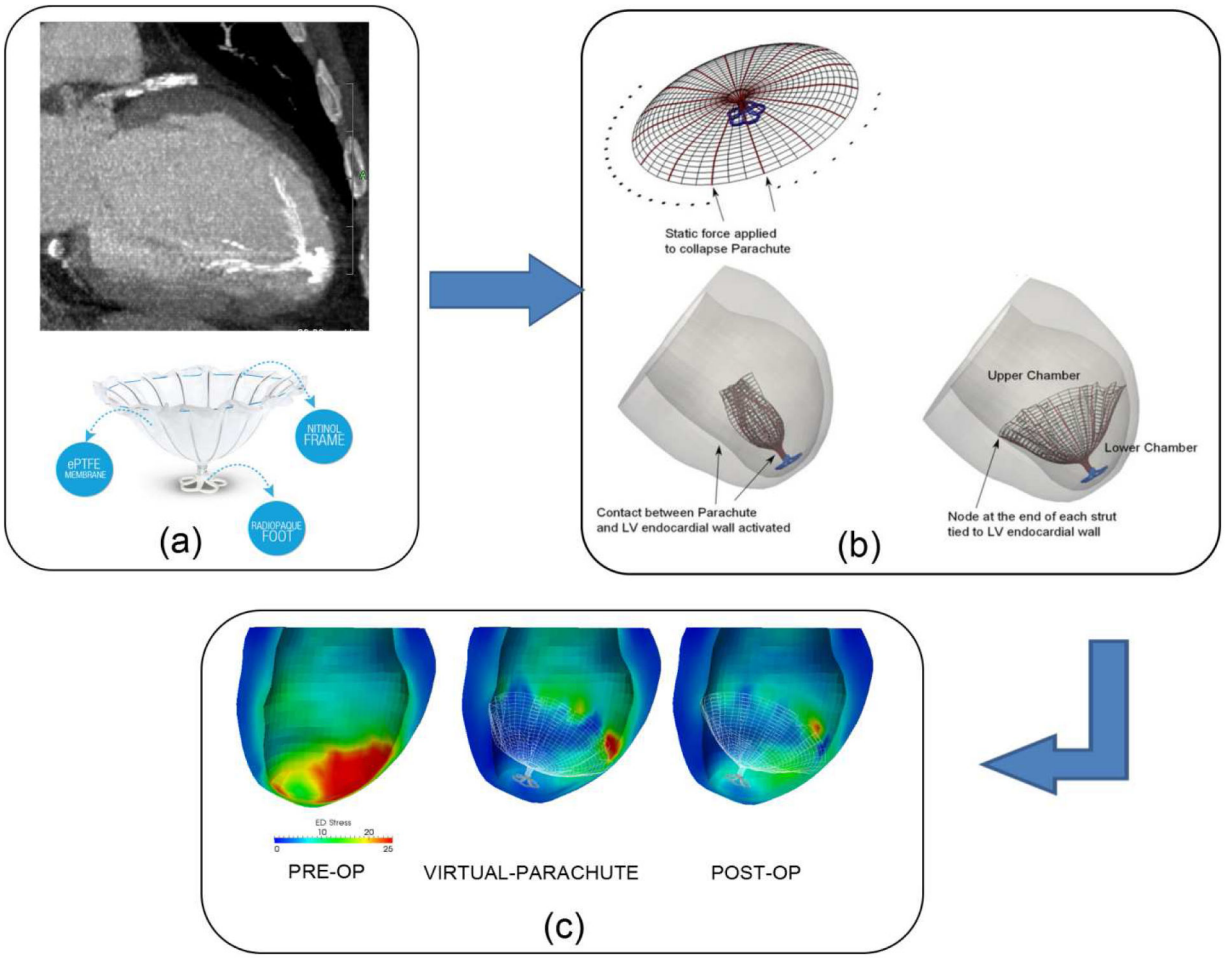

Figure 2.

Simulation of the Cardiokinetix Parachute Device. (a) Upper: CT image of the Parachute device implanted in a patient. Lower: the Parachute device. (b) Simulating the deployment of the Parachute device in the FE model. (c) Comparison of the LV myofiber stress distribution at ED before and after treatment.

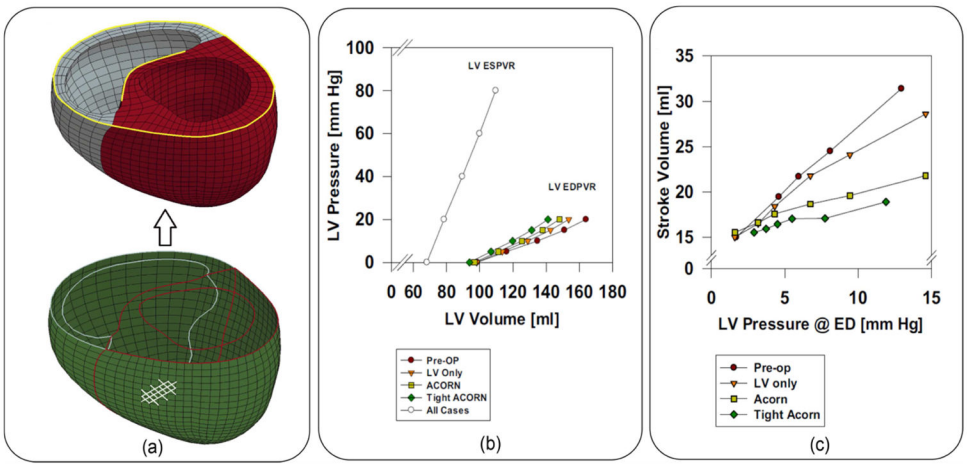

Figure 3.

Simulation of the Acorn CorCap CSD. (a) Upper: biventricular FE model showing the LV in red and right ventricle in grey. Lower: CSD model before attachment to the biventricular model as outlined by the red and gray lines. Criss-cross white lines indicate the CSD fiber orientations. (b) Effects of CSD on ED and ES pressure-volume relationships. (c) Effects of CSD on Starling's relationships. "Tight ACORN" refers to the case when a 5% pre-stretch was applied to the CSD and "LV-Only" refers to the case when the CSD encircles only the LV.

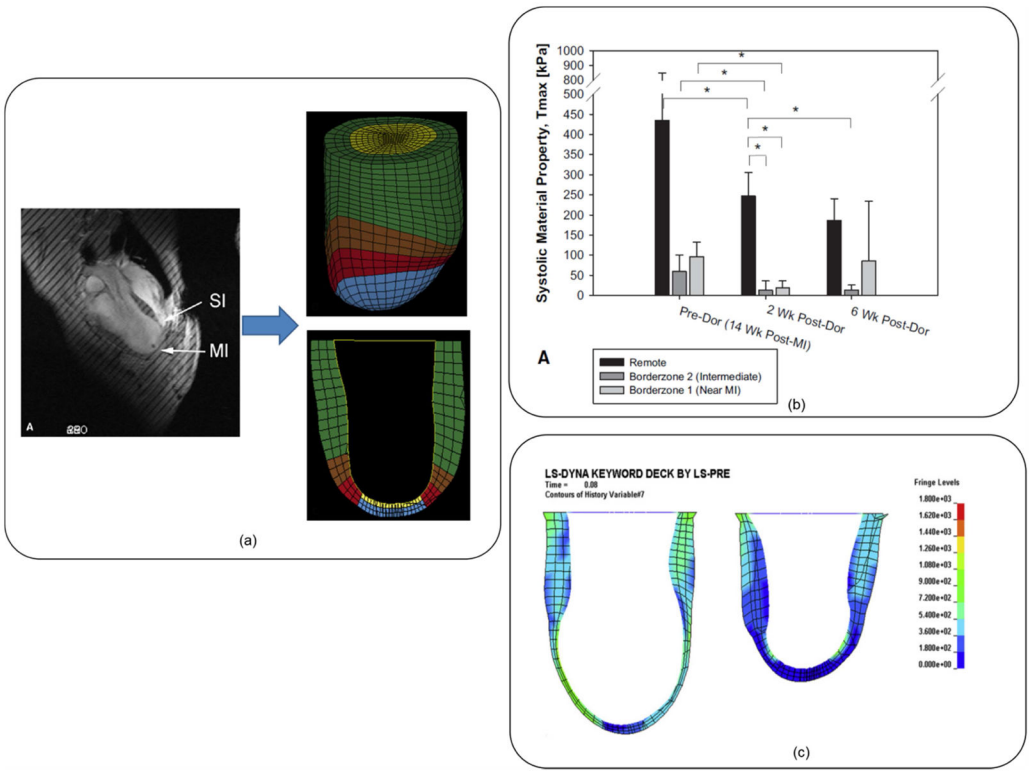

Figure 4.

Simulation of the Dor procedure. (a) Left: magnetic resonance image showing the long-axis view of the sheep LV after MI. MI and SI denote the dyskinetic and septal infarct, respectively. Tagged lines used to compute the myocardial strain can also be seen in the image. Top right: FE model of the LV. Bottom right: view of a cross section slice of the FE model. Blue, red, brown and green regions denote the infarct, the BZ 1, BZ 2 and the remote region, respectively. (b) Effects of Dor procedure on the regional myocardial contractility as reflected by the systolic material parameter. (c) Effect of Dor procedure on the longitudinal and transmural distributions of end-systolic myofiberstress pre-Dor (left) and 6weeks post-Dor (right) in a typical sheep. Fringe level units in hPa.

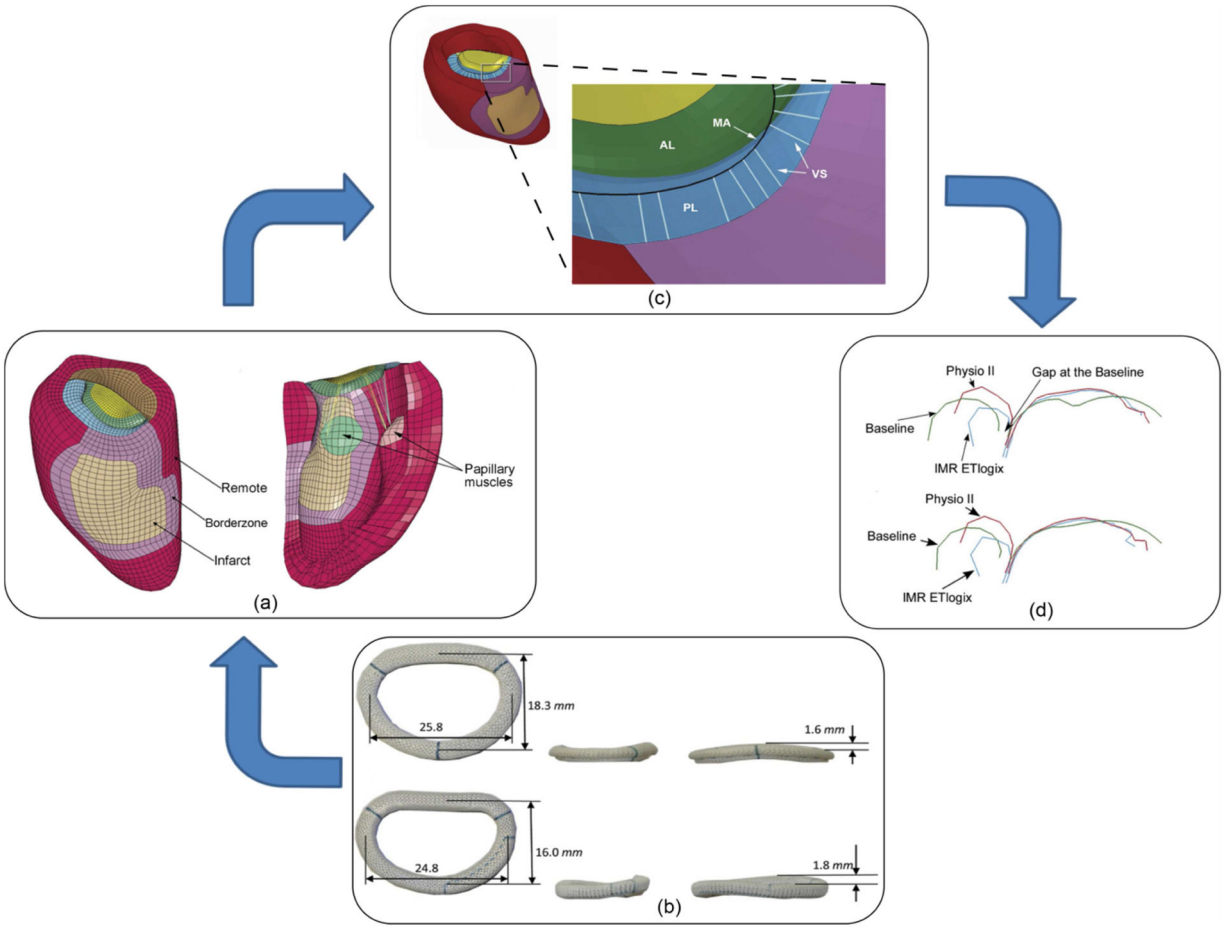

Figure 5.

Simulation of mitral valve annuloplasty. (a) FE model of the LV with the mitral valve apparatus i.e. mitral valve leaflets, chordae tendinae and the papillary muscle. (b) Annuloplasty rings with different shapes (from Edward Lifesciences, Inc, Irvine, CA). Top: saddle shape ring (Physio II). Bottom: asymmetric ring (IIMR ETlogix). (c): Annuloplasty ring virtually sutured to the mitral annulus (MA). Tension is imposed in the virtual suture (VS, shown here without tension) so that MA is pulled towards annuloplasty ring (AL = anterior leaflet, PL = posterior leaflet). (d): Improvement of the mitral leaflet coaptation after mitral annuloplasty.